HHS Public Access

Author manuscript

J Invest Dermatol. Author manuscript; available in PMC 2022 March 15.

Published in final edited form as:

J Invest Dermatol. 2021 December ; 141(12): 2876–2884.e4. doi:10.1016/j.jid.2021.03.035.

Genotype-structurotype-phenotype correlations in pachyonychia congenita patients

Tiffany T. Wu[1], **Sherif A. Eldirany**[2], **Christopher G. Bunick, MD PhD**[2], **Joyce Teng, MD PhD**[1]

[1]Department of Dermatology, Stanford University, Palo Alto, CA

[2]Department of Dermatology, Yale University, New Haven, CT

Abstract

Pachyonychia congenita (PC) is a genetic disorder of keratin that presents with nail dystrophy, painful palmoplantar keratoderma, and other clinical manifestations. We investigated genotype-structurotype-phenotype correlations seen with mutations in keratin genes (*KRT6A*, *KRT6B*, *KRT6C*, *KRT16*, *KRT17*) and utilized protein structure modeling of high frequency mutations to examine the functional importance of keratin structural domains in PC pathogenesis. Participants of the International PC Research Registry underwent genetic testing and completed a standardized survey on their symptoms. Our results support prior reports associating oral leukokeratosis with *KRT6A* mutations, and cutaneous cysts, follicular hyperkeratosis, and natal teeth with *KRT17* mutations. Painful keratoderma was prominent with *KRT6A* and *KRT16* mutations. Nail involvement was most common in *KRT6A* and least common in *KRT6C* patients. Across keratin subtypes, patients with coil 2B mutations had greatest impairment in ambulation, while patients with coil 1A mutations reported more emotional issues. Molecular modeling demonstrated that hotspot missense mutations in PC largely disrupted hydrophobic interactions or surface charge. The former may destabilize keratin dimers/tetramers, while the latter likely interferes with higher-order keratin filament formation. Understanding pathologic alterations in keratin structure improves our knowledge of how PC genotype correlates with clinical phenotype, advancing insight into disease pathogenesis and therapeutic development.

Keywords

pachyonychia congenita; mutation; genes; keratins; genotype; phenotype; structure; structurotype

Corresponding Author: Joyce Teng, MD PhD, Department of Dermatology, Stanford University, 700 Welch Road, Palo Alto, CA 94305, Tel: (650) 723-6493, jteng3@stanford.edu.

AUTHOR CONTRIBUTIONS

Tiffany T. Wu: Conceptualization, Methodology, Writing – Original draft preparation, Visualization. **Sherif A. Eldirany:** Software, Writing – Review & Editing, Visualization. **Christopher G. Bunick:** Software, Writing – Review & Editing, Visualization, Supervision. **Joyce Teng:** Conceptualization, Writing – Review & Editing, Supervision.

CONFLICT OF INTEREST

The authors have no conflicts of interest to disclose.

INTRODUCTION

Pachyonychia congenita (PC) is a rare, autosomal dominant keratin disorder caused by mutations in one of five keratin genes: *KRT6A, KRT6B, KRT6C, KRT16, or KRT17*. The disorder is commonly characterized by nail dystrophy, painful palmoplantar keratoderma, oral leukokeratosis, pilosebaceous cysts, and follicular hyperkeratosis (Fig. 1). Onset and severity of PC varies depending on the keratin gene affected, as well as the nature of the specific genetic changes caused by the mutation. Historically, mutations in *KRT6A* and *KRT16* were known as PC-1, whereas mutations in *KRT6B* and *KRT17* were known as PC-2. Recent studies showed that *KRT6A* mutations may be associated with a more severe phenotype (Spaunhurst et al., 2012), and a new classification system based on mutant gene (PC-KRT6a, PC-KRT16, etc.) was proposed (Wilson et al., 2011).

Keratins are the major structural proteins that form an intermediate filament (IF) cytoskeletal network in epithelial cells, thus playing an important role in maintaining the integrity of the epidermis, in addition to regulation of cell growth and migration. Keratins are divided into two types: the smaller (40–64 kDa) acidic type I (e.g., 6a, 6b, 6c), and the larger (52–70 kDa) basic type II (e.g., 16, 17) keratins (Chamcheu et al., 2011). They are encoded by 54 evolutionarily conserved genes (28 for type I and 26 for type II) and regulated in a pairwise and tissue differentiation-specific manner. Equal molarities of the two types of keratins form a heterodimer with a coiled-coil structure in parallel orientation. Dimerized keratins interact with each other along their lateral surface in anti-parallel orientation to form tetramers, which then associate further to build the mature IF. Regardless of their heterogeneities, all keratins contain a central alpha-helical “rod” domain flanked by non-helical “head” and “tail” domains at the amino and carboxyl termini, respectively. The central coiled-coil rod domain in keratins consists of the four alpha-helical segments 1A, 1B, 2A, and 2B, which are connected by non-helical linkers L1, L1/2, and L2, although L2 has helix potential based on hendecad repeats and vimentin and lamin crystal structures. (Ahn et al., 2019; Nicolet et al., 2010; Parry, 2006).

Rod domain boundaries consist of highly conserved 15–20 amino acid regions that are crucial for polymerization and frequently mutated in human disease (Fig. 2). Previous studies determined the majority of pathogenic variants in PC exist within these helix boundary motifs in coil 1A and 2B. Most of these mutations are missense mutations, with fewer in-frame insertions or deletions. Milder PC phenotypes have been associated with N125S and R127C mutations in *KRT16* (focal non-epidermolytic palmoplantar keratoderma, FNPPK) and N92H, R94H, and R94C mutations in *KRT17* (steatocystoma multiplex). Relatively late-onset PC (called PC-tarda) has been associated with K354N in the 2B domain of *KRT16* (Connors et al., 2001) and N109D in the 1A domain of *KRT17* (Smith, 2004; Xiao et al., 2004; McLean et al., 2005). It has been hypothesized that amino-acid substitutions causing larger, more disruptive changes to the *KRT16* protein structure would be associated with more severe disease phenotypes in PC patients with *KRT16* mutations (Fu et al., 2011).

In this study, we identify clinically significant PC mutations in each of the keratin genes and correlate the specific genetic changes with clinical manifestations, as well as functional and

emotional impacts on PC patients' quality of life. Knowledge about specific gene mutations that patients carry and the associated phenotype will provide insights to disease pathogenesis and progression and thus guide clinical management. To place these clinicopathologic findings into a molecular context, we characterized the alterations to the keratin structure caused by each PC mutation (the "PC structurotype"), thereby connecting genetic mutation, protein structure, and clinical phenotype. Ultimately, understanding genotype-structurotype-phenotype correlations may help guide development of targeted therapies for patients with this challenging disorder, as well as other keratinopathies.

RESULTS

As of January 2020, the International PC Research Registry (IPCRR) contained genetic and survey data on over 700 PC patients. Over half of these patients (54%) had confirmed *KRT6A* mutations (n=383), 12% had *KRT6B* (n=89), 4% had *KRT6C* (n=31), 9% had *KRT16* (n=61), and 21% had *KRT17* (n=150).

Keratin Gene Mutations in PC

Specific mutations identified in each keratin gene were mapped according to domain positions previously reported (Szeverenyi et al., 2008). In our registry, most PC patients had a mutation in either keratin coil 1A or coil 2B, especially within the conserved boundary region (Fig. 2). The mutations include both substitutions and deletions. Among those carrying mutations within *KRT6B* and *KRT6C*, the mutations are frequently found in the coil 2B domain. The mutations within *KRT6A*, *KRT16*, and *KRT17*, on the other hand, are frequently found in the coil 1A domain. A few patients had mutations in the head region of *KRT6A* (n=9) and *KRT16* (n=2), while tail (n=18) mutations were only seen in *KRT6A* patients. Of note, no mutations were observed in the linkers or in coils 1B or 2A (Fig. 2).

Fifty-six unique variations were seen in patients with *KRT6A* mutations, 6 in *KRT6B*, 4 in *KRT6C*, 16 in *KRT16*, and 20 in *KRT17*. N172del (n=109) was the most common *KRT6A* mutation. This same mutation was the second most common *KRT6B* mutation seen (n=26) and third most common mutation *KRT6C* mutation seen (n=5). E472K also was a common mutation seen in *KRT6A* (n=19), *KRT6B* (n=52), and *KRT6C* (n=15) patients. N125S (n=17) was the most commonly seen mutation in *KRT16* patients, followed by R127C (n=13); both mutations were previously reported to have a milder phenotype in PC patients (FNPPK) (McLean et al., 2005) (Supplemental Tables).

Phenotype Correlations by Gene

We examined the presence and severity of common clinical manifestations of PC across *KRT* gene groups. Although palmoplantar keratoderma is a common clinical feature among PC patients, it is most prevalent among *KRT16* patients, with 58% palmar and 100% plantar involvement. *KRT17* patients are less affected, with 17% palmar and 70% plantar keratoderma in comparison. Plantar keratoderma in general is more severe than palmar symptoms, likely due to weight bearing (Table 1).

Oral leukokeratosis is most prominent in *KRT6A* patients (87%), while skin findings (including cysts and follicular hyperkeratosis) are most common in *KRT17* patients (76%

and 61%, respectively). Natal or prenatal teeth were also seen predominantly in *KRT17* patients (76% incidence). Alopecia was seen at a relatively similar incidence across the *KRT* genes. Hyperhidrosis had a higher incidence than alopecia, affecting at least 20% of patients in all *KRT* gene groups (Table 2).

Nail involvement in PC varies by genotype. While onychodystrophy affects most of the *KRT6A* patients (96% with definite or likely fingernail involvement), this is much less common (3%) among those with *KRT6C* mutations. The severity of the onychodystrophy in the *KRT6A* group was also reflected by the percentage (10%) of patients who have had surgical interventions in at least 1 fingernail, while no *KRT6C* patients required surgery. Similar patterns were seen with toenail involvement, with 97% in *KRT6A* patients, in comparison to 19% in *KRT6C* patients. Overall prevalence of nail thickening was higher in toenails than fingernails. More *KRT6B* patients with toenail dystrophy elect to have surgery (16%), in comparison to those with *KRT17* (11%) and *KRT6A* (9%) mutations (Fig. 3).

Functional and Emotional Impact of PC

Greater than 60% of patients report severe functional impairment due to pain while ambulating or the requirement of a walking aid to ambulate (Fig. 4). This appears to be more prevalent when mutations occur in coil 2B (range across keratin subgroups: 85–100%) compared to coil 1A (range: 60–92%). Functional impairment was reported most frequently by *KRT16* patients with 1 out of 2 patients (50%) in the head region, 46 out of 53 (92%) in coil 1A, and 6 out of 6 (100%) in coil 2B reporting pain with walking or inability to walk without a walking aid.

In addition, more than eighty percent of patients with *KRT6C* or *KRT16* mutations reported painful plantar keratoderma regardless of ambulation. These individuals reported “pain often requires medication” or “very painful but no medication” (Zieman and Coulombe, 2020; Weinberg et al., 2020). Although these complaints are less prevalent in *KRT17* patients, they still affect about 50% of the cohort (Fig. 3). Painful keratoderma is linked to significant emotional or psychiatric stress in over a quarter of patients in all *KRT* groups except *KRT6C* (Fig. 4).

Molecular Modeling of Coil 1A Mutations

The structural alterations to the keratin protein caused by missense mutations were analyzed using three-dimensional computational modeling. The F174S variant seen in 21 *KRT6A* patients eliminates an aromatic-aromatic stacking interaction with Y131 in K16 at the interface of the K6A/K16 keratin dimer. This likely destabilizes the protein-protein interaction by reducing the strength of hydrophobic bonds (Fig. 5A). F174S also disrupts a hydrophobic patch on the protein surface of the N-terminal aspect of the rod domain, thereby possibly interfering with higher-order keratin filament interactions (Fig. 5B).

$N171^{K6A}$ is located on the exposed surface of the K6/K16 dimer rather than in the occluded dimer interface; therefore, mutations of this residue are not predicted to affect K6/K16 dimerization during filament assembly (Fig. 5A). $N171K^{K6A}$ increases the basic charge at the N-terminus of the molecule, thereby potentially altering higher-order IF assembly (Fig. 5C). On the other hand, $N171S^{K6A}$ does not cause any significant change in surface

hydrophobicity or charge (as expected for a polar-to-polar mutation), but does reduce residue size and thus may affect higher-order interactions.

Following generation of these structural models, we examined the clinical presentation of patients with N171S compared to those with F174S to determine if phenotype may be less severe when there are no changes to hydrophobicity or charge. Compared to patients with a F174S mutation, keratin 16 patients with N171S appear to have less pain associated with plantar keratoderma (62.5% vs. 84.2%), as well as a much lower incidence of emotional or psychiatric issues (9.1% vs. 61.1%) (Supplemental Table 6). Based on this, we hypothesize that uncontrolled pain from plantar keratoderma may be a large contributing factor to the development of emotional or psychiatric issues in PC patients.

Since $N125^{K16}$ and $N92^{K17}$ are in homologous positions on their respective genes, the mutations $N125S^{K16}$ and $N92S^{K17}$ have similar structural effects. Like $N171S^{K6A}$, the polar-to-polar mutation in these surface-exposed residues is not predicted to affect the dimer interface or substantially alter surface characteristics, but would reduce residue size (Supplemental Fig. 1A).

The second most common mutation in *KRT16* patients was R127C, which decreases residue size and reduces basic charge at the N-terminus of the 1A domain (Fig. 5A,D). The introduction of cysteine creates the potential for aberrant disulfide cross-linking between keratin subunits. L99P is the second most common mutation in *KRT17* patients, which eliminates hydrophobic interactions, particularly with $F177^{K6A}$, thereby destabilizing the K6A/K17–1A dimer (Fig. 5E). Such disruption of the keratin dimer interactions may interfere with higher-order IF formation and its mechanical strength (Fig. 5F).

Based on these analyses, we hypothesized that keratin 17 patients with L99P mutation may have a more severe phenotype than those with N92S mutation. Nail involvement of both fingers and toes were more prevalent in L99P patients compared to those with N92S (100% vs. 70.5% and 100% vs. 93.4%, respectively) (Supplemental Table 7). Skin findings, including cysts and follicular hyperkeratosis, occurred at a higher incidence in patients with L99P (81.3% vs. 67.2% and 75% vs. 47.5%, respectively). Hyperhidrosis was also more common in L99P patients compared to N92S patients (50% vs. 25%).

Molecular Modeling of Coil 2B Mutations

To analyze structural alterations in the keratin 2B domain caused by PC mutations, we generated K6A/K16–2B and K6A/K17–2B structural models. Several important mutations in the conserved C-terminus of K6A, K16, and K17 are modeled in comparison. L469P, observed in 14 *KRT6A* patients, reduces the hydrophobicity of a surface-exposed hydrophobic patch at the C-terminus of the 2B domain (Fig. 5G,I). Notably, this mutation is in the conserved TYR*LLEGE motif known to be important for higher-order filament assembly (Lomakin et al., 2020; Wilson et al., 1992). $E472K^{K6A}$ is commonly seen in *KRT6A*, *KRT6B*, and *KRT6C* patients and reduces the acidic charge at the 2B domain C-terminus within the TYR*LLEGE motif in each of these keratins (Fig. 5G,H).

I462N and A463P were observed in 9 *KRT6A* patients. I462N^{K6A} reduces hydrophobic interactions with L410 and Y417 at the K6A/K16 dimer interface. A463P does not significantly alter residue charge or polarity of the mutation site, but proline substitution is bulkier and likely causes helix kinking of K6A (Supplemental Fig. 1B,C). Since A463P immediately precedes the TYR*LLEGE motif, the helix disruption by proline substitution could significantly alter the motif's function in promoting key subunit interactions needed for IF formation. Similar structural alteration likely occurred due to R418P mutation seen in 5 *KRT16* patients. The proline substitution not only reduces basic charge at the surface of the 2B C-terminus (Supplemental Fig. 1D), but also disrupts the protein backbone due to kinking within the TYR*LLEGE motif. L388P, which was present in 9 *KRT17* patients, eliminates hydrophobic interactions with L468^{K6A} and Y465^{K6A} at the dimer interface (Supplemental Fig. 1E,F). This mutation is also in the conserved TYR*LLEGE motif and is predicted to have detrimental impact like A463P^{K6A}, L469^{K6A}, and R418^{K16}.

Though limited in patient numbers, we compared clinical characteristics of patients with L469P (which is within the TYR*LLEGE motif) and those with A463P (which precedes the motif) to examine whether mutations within the motif may have more severe phenotype. Though relatively similar percentages of patients reported pain with ambulation (80.0% vs. 83.3%), of those patients whose walking is affected by PC, more patients with L469P (33.3%) reported being able to walk less than 1 city block, while all A463P patients could walk at least 1 city block (Supplemental Table 8). Furthermore, a higher percentage of patients with L469P reported use of a walking aid (40.0% vs. 16.7%).

DISCUSSION

PC is a complex genetic disorder with high variability in phenotype. The spectrum of mutations seen in PC is also extensive. In our cohort, 56 unique mutations were seen in *KRT6A* patients, 6 in *KRT6B*, 5 in *KRT6C*, 16 in *KRT16*, and 20 in *KRT17*. Examples of keratin structural alteration due to the mutations were demonstrated via molecular modeling. Analysis of the clustering of the mutations also allowed us to evaluate the functional importance of different structural domains within each keratin. Although we cannot rule out the possibility of founder's effect, many of the PC patients in our registry carry mutations in the coil 1A and 2B domains, especially along the boundary of these domains, suggesting that these regions are of particular functional importance.

Molecular modeling revealed that many of the missense mutations causing PC occur in residues that are predicted to be surface-exposed in the keratin dimer, which means their mutation can alter the surface properties of the keratins. Our data showed that fewer PC mutations exist in the hydrophobic core of the keratin dimers, with only 8/19 of the most common PC 1A/2B missense mutations (Supplemental Tables 1–5) occurring in heptad repeat positions a or d (the major positions usually contributing to the hydrophobic dimer interface), although some residue positions contribute to dimer interface, have solvent-accessible surface area, and are not hydrophobic. It is thus likely that the predominant disease mechanism involves disruption of intermolecular interactions responsible for higher-order (tetramer or higher) keratin filament assembly, while destabilization of keratin dimers by elimination of hydrophobic interactions at the dimer interface is less common in the

population. This is supported by the observation that the coil 2B mutations cluster around the conserved TYR*LLEGE motif at the 2B C-terminus that is known to be critical for intermolecular interactions regulating the lateral alignment of intermediate filament assembly (Wilson et al., 1992). Several helix-breaking proline substitutions in the 2B C-terminus (L469P^{K6A}, A463P^{K6A}, R418P^{K16}, L388P^{K17}) suggest that the structure of this region is important for both keratin dimerization and intermediate filament assembly. The other coil 2B mutation occurring with high frequency, E472K^{K6A}, causes a dramatic reduction in 2B C-terminus acidity, suggesting that the region's charge is also critical for protein function. Based on our genotype-structurotype-phenotype correlation analyses, our results support the hypothesis that mutations affecting higher order filament assembly may be associated with a more severe phenotype in PC.

It would be useful to have an algorithm that accurately correlates PC patient genotype with the protein structure perturbations and severity of clinical phenotype. Due to a knowledge gap about the precise molecular interactions that govern higher-order/mature intermediate filament assembly (cite Eldirany SA, Lomakin IB, Ho M, Bunick CG. Curr Opin Cell Biol. 2020), we found that it was not possible at the current time to create an accurate *a priori* predictive algorithm for novel PC variants and clinical phenotype/severity. For example, oral leukokeratosis due to K6a mutation and natal teeth due to K17 mutation can occur with mutations in either the 1A or 2B subdomains (Figure 2c). The molecular mechanism of how 1A and 2B subdomains contribute to mature keratin IF assembly is still not understood, and this limits computational prediction accuracy. Despite this knowledge gap, an algorithm that attempts to predict keratin variant pathogenicity without utilizing higher-order molecular contact information was recently developed (cite Ying et al, Human Genomics, 2020, entitled "KVarPredDB: a database for predicting pathogenicity of missense sequence variants of keratin genes associated with genodermatoses"), and represents one step forward in our capacity to improve the computational correlation of genotype, structure, and pathogenicity.

Importantly, our analysis of pathogenic PC mutations has similarities to prior studies of K5 or K14 mutations causing epidermolysis bullosa simplex (EBS) [cite DOI: 10.1038/nsmb.2330; and DOI: 10.1039/c4mb00138a]. Both PC and EBS demonstrate that basic biochemical fundamentals like hydrophobic contacts, electrostatic interactions, hydrogen bonds, steric hindrance, and physico-chemical amino acid properties matter immensely for the proper dimer, tetramer, and higher-order oligomeric assembly of IFs. Like PC, analysis of EBS-causing mutations demonstrated that many mutations occur in the 1A and 2B subdomains, with special clustering in and around the TYR*LLEGE motif in the C-terminus of the 2B subdomain. As noted, the TYR*LLEGE motif contains molecular contacts critical for higher-order keratin IF assembly (cite Lomakin et al 2020 and Wilson et al 1992 already in our REF list, and add Lee…Coulombe 2020 10.1016/j.str.2020.01.002). Interestingly, however, the severity of disease phenotype for PC or EBS (cite DOI: 10.1039/c4mb00138a) varies from mild to severe even from mutations within the TYR*LLEGE motif, reflecting the heterogeneity of clinical phenotype among keratinopathies even when mutations are clustered in a conserved functional region. The existence of two different disease types (PC and EBS) heavily linked to the 1A and 2B subdomains indicates those subdomains have an important, conserved function across the keratin family. Which keratinopathy a patient

manifests, therefore, depends on the specific keratin gene altered and in which tissue the abnormal keratin is expressed, with the severity of phenotype less predictable but potentially correlated with local biochemical changes caused by mutation.

Our phenotype analysis is consistent with previous literature reporting associations of oral leukokeratosis with *KRT6A* mutations, and the presence of natal teeth with *KRT17* mutations [Smith et al., 2006]. Finally, self-reported functional and emotional impact by the registry participants indicated that PC is a progressive and debilitating disease that greatly affects quality of life for affected individuals. The majority of patients in this study reported either an inability to walk without pain or the frequent need for walking aids. Additionally, emotional or psychiatric issues were noted in many of these patients. Our results indicate coil 2B mutations may be associated with more severe functional impairment (based on ability to ambulate), while coil 1A mutations may be associated with more severe emotional distress in PC patients. Overall, these results emphasize the high burden of disease in PC patients and current unmet medical needs.

As there is no FDA-approved treatment for this disease, current PC therapy focuses on symptomatic management of disease manifestations, including keratoderma, pain due to skin fragility, fissures, as well as secondary skin infections. For example, pain from plantar keratoderma is primarily addressed by frequent paring, reducing weight bearing, friction and trauma avoidance to the feet, softening calluses with skin emollients, and minimizing skin blistering by controlling hyperhidrosis. Nail dystrophy is typically managed via frequent trimming and surgical removal when severely symptomatic. Oral leukokeratosis usually remains asymptomatic with good oral hygiene and gentle daily care by brushing with a soft toothbrush. Secondary fungal and bacterial infections are commonly attributed as a cause of pain.

Several clinical trials using targeted therapies are in progress. Statins were previously demonstrated to downregulate *KRT6A* promoter activity (Zhao et al., 2011) and reduce aberrant protein production. An ongoing Phase III study using a topical mTOR inhibitor is being evaluated for every subtype of PC patients. Short interfering RNA (siRNA) can selectively block expression of specific *K6A*-pathogenic variant (Hickerson et al., 2009; Leachman et al., 2008) and has been used to treat a *K6A* patient with N171K mutation (Leachman et al., 2010). In addition, botulinum toxin has been used to treat hyperhidrosis, a frequent cause of pain in PC patients, with promising results (Swartling and Vahlquist, 2006; Swartling et al., 2010; González-Ramos et al., 2016). Other therapies that have been investigated include anti-TNF biologics, gabapentin, duloxetine/tricyclics, and capsaicin injections.

Prior study in keratin 16 null mice has suggested the role of oxidative stress and dysfunctional nuclear factor erythroid-derived 2 related factor 2 (NRF2) in the pathophysiology of palmoplantar keratoderma lesions (Kerns et al., 2016; Kerns et al., 2018; Zieman et al., 2019; Zieman and Coulombe, 2020). Notably, topical application of the NRF2 activator sulforaphane to the footpad of mice null for keratin 16 prevented development of palmoplantar keratoderma. The results from these studies contribute to our understanding of

palmoplantar keratoderma in PC disease and may provide insights into future therapeutics that may be promising in humans.

Our study represents the largest genotype-phenotype correlation analysis of PC to date, with added emphasis on delineating the structural alterations due to these mutations (Eldirany et al., 2020; Lomakin et al., 2020). Limitations of this study include the inability to perform molecular modeling on patients with deletion mutations; such genetic change certainly may harm keratin structure. Nonetheless, our study has epitomized the approach to investigate a rare monogenetic disorder by understanding the genotype-structurotype-phenotype correlation, which will help delineate disease pathogenesis, manifestation and progression, ultimately guiding our clinical management of PC patients.

MATERIALS & METHODS

The data utilized in this study were obtained through the International PC Research Registry (IPCRR), which was established in 2004. The registry was approved by the Western Institutional Review Board (no. 20040468) (see more details at www.pachyonychia.org). Subjects who participated in the registry underwent genetic testing (Smith et al., 2005) and completed a standardized survey, which included questions on the presence and severity of PC clinical manifestations such as palmoplantar keratoderma, nail thickening, oral leukokeratosis, and skin/hair abnormalities. Questions on patient-reported pain and its impact on patients' ability to walk, as well as emotional/psychiatric issues were also included (Supplemental).

Structural models of the K6A/K16–1A, K6A/K16–2B, K6A/K17–1A, and K6A/K17–2B heterodimers were generated using the SWISS-MODEL homology-modeling server (Waterhouse et al., 2018). Templates were chosen based on Global Model Quality Estimation (GMQE) scores; the 1A models were generated using the K1/K10 coil 2B (Cys401Ala) crystal structure (PDB ID: 6UUI), while 2B models used wild-type K1/K10 coil 2B crystal structure (PDB ID: 4ZRY) (Bunick and Milstone, 2017; Lomakin et al., 2020). There currently is no experimentally determined heteromeric keratin 1A structure. All models were energy-minimized using UCSF Chimera (Pettersen et al., 2004). Structure analysis was performed using UCSF Chimera and the Adaptive Poisson-Boltzmann Solver (APBS) server (Baker et al., 2001).

Data Availability

Datasets related to this article were obtained from the Pachyonychia Congenita Project; data summaries of the IPCRR are available at www.pachyonychia.org/pc-data/.

Supplementary Material

Refer to Web version on PubMed Central for supplementary material.

ACKNOWLEDGEMENTS

We thank Holly Evans and Janice Schwartz from the Pachyonychia Congenita Project for their generous support of this project, as well as all the PC patients who participated in the registry. This work was supported by the Richard

K. Gershon, M.D., Student Research Fellowship at Yale University School of Medicine (to SAE), and National Institutes of Health/National Institute of Arthritis and Musculoskeletal and Skin Disorders Awards K08AR070290 and R03AR076484 (to CGB).

REFERENCES

1. Ahn J, Jo I, Kang SM, Hong S, Kim S, Jeong S, et al. Structural basis for lamin assembly at the molecular level. Nat Commun 2019;10(1):3757. [PubMed: 31434876]
2. Baker NA, Sept D, Joseph S, Holst MJ, McCammon JA. Electrostatics of nanosystems: application to microtubules and the ribosome. Proc Natl Acad Sci USA. 2001;98:10037–41. [PubMed: 11517324]
3. Bunick CG, Milstone LM. The x-ray crystal structure of the keratin 1-keraton 10 helix 2B heterodimer reveals molecular surface properties and biochemical insights into human skin disease. J Invest Dermatol. 2017;137(1):142–150. [PubMed: 27595935]
4. Chamcheu JC, Siddiqui IA, Syed DN, Adhami VM, Liovic M, Mukhtar H. Keratin Gene Mutations in Disorders of Human Skin and its Appendages. Arch Biochem Biophys. 2011;508:123–137. [PubMed: 21176769]
5. Connors JB, Rahil AK, Smith FJ, McLean WH, Milstone LM. Delayed-onset pachyonychia congenita associated with a novel mutation in the central 2B domain of keratin 16. Br J Dermatol. 2001;144:1058–62. [PubMed: 11359398]
6. Eldirany SA, Ho M, Bunick CG. The Interface between Keratin Structurotype and Human Disease. Structure. 2020;28:271–3. [PubMed: 32130887]
7. Fu T, Leachman SA, Wilson NJ, Smith FJ, Schwartz ME, Tang JY. Genotype-phenotype correlations among pachyonychia congenita patients with K16 mutations. J Invest Dermatol. 2011;131:1025–8. [PubMed: 21160496]
8. González-Ramos J, Sendagorta-Cudós E, González-López G, Mayor-Ibarguren A, Feltes-Ochoa R, Herranz-Pinto P. Efficacy of botulinum toxin in pachyonychia congenita type 1: report of two new cases. Dermatol Ther. 2016;29:32–6. [PubMed: 26445325]
9. Hickerson RP, Leake D, Pho LN, Leachman SA, Kaspar RL. Rapamycin selectively inhibits expression of an inducible keratin (KRT6a) in human keratinocytes and improves symptoms in pachyonychia congenita patients. J Dermatol Sci. 2009;56:82–8. [PubMed: 19699613]
10. Kerns ML, Hakim JM, Lu RG, Guo Y, Berroth A, Kaspar RL, et al. Oxidative stress and dysfunctional NRF2 underlie pachyonychia congenita phenotypes. J Clin Invest. 2016;126(6):2356–2366. [PubMed: 27183391]
11. Kerns ML, Hakim JM, Zieman A, Lu RG, Coulombe PA. Sexual Dimorphism in Response to an NRF2 Inducer in a Model for Pachyonychia Congenita. J Invest Dermatol. 2018;138(5):1094–1100. [PubMed: 29277538]
12. Leachman SA, Hickerson RP, Hull PR, Smith FJ, Milstone LM, Lane EB, et al. Therapeutic siRNAs for dominant genetic skin disorders including pachyonychia congenita. J Dermatol Sci. 2008;51:151–7. [PubMed: 18495438]
13. Leachman SA, Hickerson RP, Schwartz ME, Bullough EE, Hutcherson SL, Boucher KM, et al. First-in-human mutation-targeted siRNA phase Ib trial of an inherited skin disorder. Mol Ther. 2010;18:442–6. [PubMed: 19935778]
14. Lomakin IB, Hinbest AJ, Ho M, Eldirany SA, Bunick CG. Crystal structure of keratin 1/10(C401A) 2B heterodimer demonstrates a proclivity for the C-terminus of helix 2B to form higher order molecular contacts. Yale J Biol Med. 2020;93:3–17. [PubMed: 32226330]
15. McLean WH, Smith FJ, Cassidy AJ. Insights into genotype-phenotype correlation in pachyonychia congenita from the human intermediate filament mutation database. J Investig Dermatol Symp Proc. 2005;10:31–36.
16. Nicolet S, Herrmann H, Aebi U, Strelkov SV. Atomic structure of vimentin coil 2. J Struct Biol. 2010;170:369–76. [PubMed: 20176112]
17. Parry DA. Hendecad repeat in segment 2A and linker L2 of intermediate filament chains implies the possibility of a right-handed coiled-coil structure. J Struct Biol. 2006;155(2):370–4. [PubMed: 16713299]

18. Pettersen EF, Goddard TD, Huang CC, Couch GS, Greenblatt DM, Meng EC, et al. UCSF chimera – a visualization system for exploratory research and analysis. J Comput Chem. 2004;25:1605–12. [PubMed: 15264254]
19. Smith FJ. Nail that mutation-keratin 17 defect in late-onset pachyonychia. J Invest Dermatol. 2004;122:x–xi.
20. Smith FJ, Hansen CD, Hull PR, Kaspar RL, McLean WH, O'Tool E, et al. Pachyonychia Congenita. 2006 Jan 27 [Updated 2017 Nov 30]. In: Adam MP, Ardinger HH, Pagon RA, et al., editors. GeneReviews [Internet]. Seattle (WA): University of Washington, Seattle; 1993–2020.
21. Smith FJ, Liao H, Cassidy AJ, Stewart A, Hamill KJ, Wood P et al. The genetic basis of pachyonychia congenital. J Investig Dermatol Symp Proc. 2006;10:21–30.
22. Spaunhurst KM, Hogendorf AM, Smith FJ, Lingala, Schwartz ME, Cywinska-Bernas A, Zeman KJ, Tang JY. Pachyonychia congenita patients with mutations in KRT6A have more extensive disease compared with patients who have mutations in KRT16. Br J Dermatol. 2012;166(4):875–8. [PubMed: 22098151]
23. Swartling C, Vahlquist A. Treatment of pachyonychia congenita with plantar injections of botulinum toxin. Br J Dermatol. 2006;154:763–5. [PubMed: 16536826]
24. Swartling C, Karlqvist M, Hymnelius K, Weis J, Vahlquist A. Botulinum toxin in the treatment of sweat-worsened foot problems in patients with epidermolysis bullosa simplex and pachyonychia congenita. Br J Dermatol. 2010;163:1072–6. [PubMed: 20618323]
25. Szeverenyi I, Cassidy AJ, Chung CW, Lee BT, Common JE, Ogg SC, et al. The Human Intermediate Filament Database: comprehensive information on a gene family involved in many human diseases. Hum Mutat. 2008;29:351–60. [PubMed: 18033728]
26. Waterhouse A, Bertoni M, Bienert S, Studer G, Tauriello G, Gumienny R, et al. SWISS-MODEL: homology modelling of protein structures and complexes. Nucleic Acids Res. 2018;46:296–303.
27. Weinberg RL, Coulombe PA, Polydefkis M, Caterina MJ. Pain mechanisms in hereditary palmoplantar keratodermas. Br J Dermatol. 2020;182(3):543–551. [PubMed: 30883689]
28. Wilson AK, Coulombe PA, Fuchs E. The roles of K5 and K14 head, tail, and R/K L L E G E domains in keratin filament assembly in vitro. J Cell Biol. 1992;119:401–14. [PubMed: 1383231]
29. Wilson NJ, Leachman SA, Hansen CD, McMullan AC, Milstone LM, Schwartz ME, et al. A large mutational study in pachyonychia congenita. J Invest Dermatol. 2011;131:1018–24. [PubMed: 21326300]
30. Xiao SX, Feng YG, Ren XR, Tan SS, Li L, Wang JM, et al. A novel mutation in the second half of the keratin 17 1A domain in a large pedigree with delayed-onset pachyonychia congenita type 2. J Invest Dermatol. 2004;122:892–5. [PubMed: 15102078]
31. Zhao Y, Gartner U, Smith FJ, McLean WH. Statins downregulate KRT6a promoter activity: a possible therapeutic avenue for pachyonychia congenita.
32. Zieman AG, Coulombe PA. Pathophysiology of pachyonychia congenita-associated palmoplantar keratoderma: new insights into skin epithelial homeostasis and avenues for treatment. Br J Dermatol. 2020;182(3):564–573. [PubMed: 31021398]
33. Zieman AG, Poll BG, Ma J, Coulombe PA. Altered keratinocyte differentiation is an early driver of keratin mutation-based palmoplantar keratoderma. Human Molecular Genetics. 2019;28(13):2255–2270. [PubMed: 31220272]

Figure 1. Common clinical manifestations of PC

include (A) toenail dystrophy, (B) plantar keratoderma, (C) cysts, and (D) oral leukokeratosis. Hypertrophic nail dystrophy is the predominant clinical feature of PC, typically presenting either with nails that grow to full length but have an upward slant caused by distal hyperkeratosis, or nails with a nail plate that terminates prematurely leaving a sloping distal region of hyperkeratosis and exposed distal finger tip. Palmoplantar keratoderma, which may be associated with intense pain, is another manifestation that typically presents when a child begins walking. Dermatological manifestations of PC include pilosebaceous cysts and follicular hyperkeratosis. Oral leukokeratosis presents as thickened white patches on the tongue and cheek. Other common manifestations of PC include natal or prenatal teeth, as well as hyperhidrosis (not pictured).

a

b

		Head	1A	L1	1B	L1/2	2A	L2	2B	Tail
K6A *n*=383	Amino acids	1-163	164-198	199-210	211-311	312-328	329-347	348-355	356-476	477-564
		n=9	*n*=249	*n*=0	*n*=0	*n*=0	*n*=0	*n*=0	*n*=107	*n*=1
K6B *n*=89	Amino acids	1-163	164-198	199-210	211-311	312-328	329-347	348-355	356-476	477-564
		n=0	*n*=29	*n*=0	*n*=0	*n*=0	*n*=0	*n*=0	*n*=60	*n*=0
K6C *n*=31	Amino acids	1-163	164-198	199-210	211-311	312-328	329-347	348-355	356-476	477-564
		n=0	*n*=5	*n*=0	*n*=0	*n*=0	*n*=0	*n*=0	*n*=26	*n*=0
K16 *n*=61	Amino acids	1-117	118-152	153-163	164-264	265-280	281-299	300-307	308-428	429-473
		n=2	*n*=53	*n*=0	*n*=0	*n*=0	*n*=0	*n*=0	*n*=6	*n*=0
K17 *n*=150	Amino acids	1-84	85-119	120-130	131-231	232-247	248-266	267-274	275-395	396-432
		n=0	*n*=141	*n*=0	*n*=0	*n*=0	*n*=0	*n*=0	*n*=9	*n*=0

C

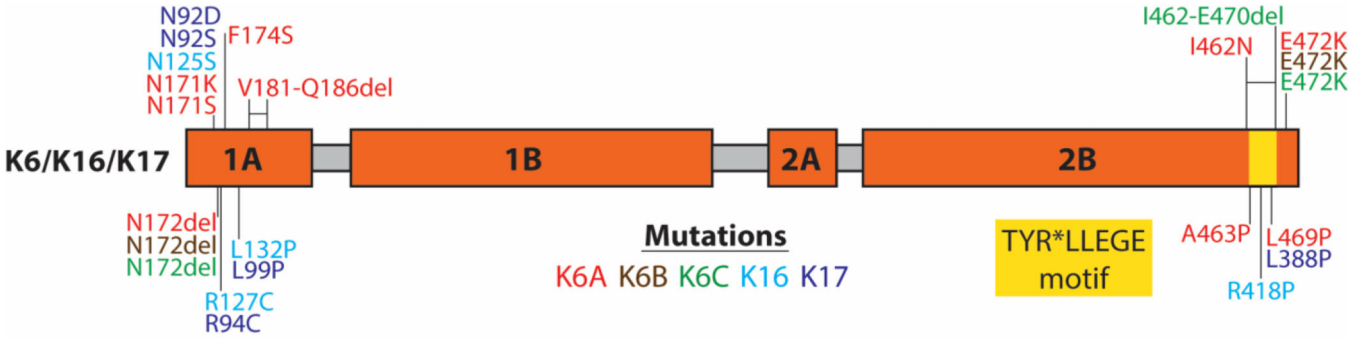

Figure 2. Mutations by KRT Gene Location

(A) Schematic of the domain structure of the keratin protein. Sequence domains were obtained from the Human Intermediate Filament Database (interfil.org). (B) The number of amino acid residues and patients with mutations located in each subdomain. (C) Mapping of PC missense mutations onto the keratin domain structure.

a Fingernail involvement

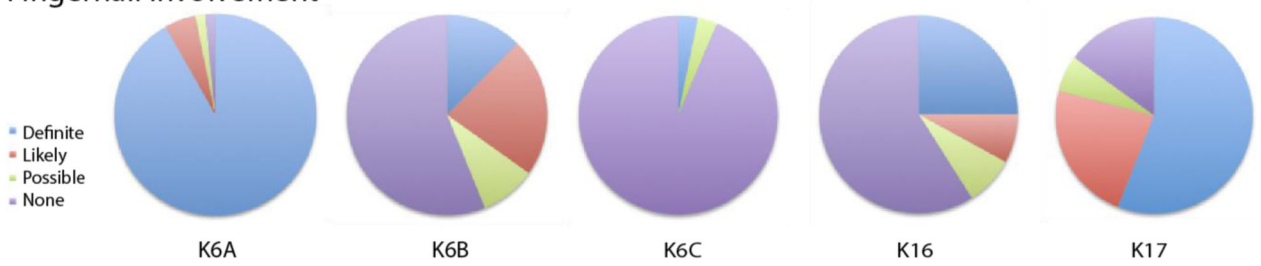

Number of fingernails surgically removed

	KRT6A	KRT6B	KRT6C	KRT16	KRT17
>7 nails	25 (7%)	0 (0%)	0 (0%)	6 (2%)	2 (1%)
4-6 nails	5 (1%)	1 (1%)	0 (0%)	2 (1%)	1 (1%)
1-3 nails	8 (2%)	4 (4%)	0 (0%)	14 (4%)	3 (2%)
None	345 (90%)	84 (94%)	31 (100%)	292 (93%)	145 (96%)

b Toenail involvement

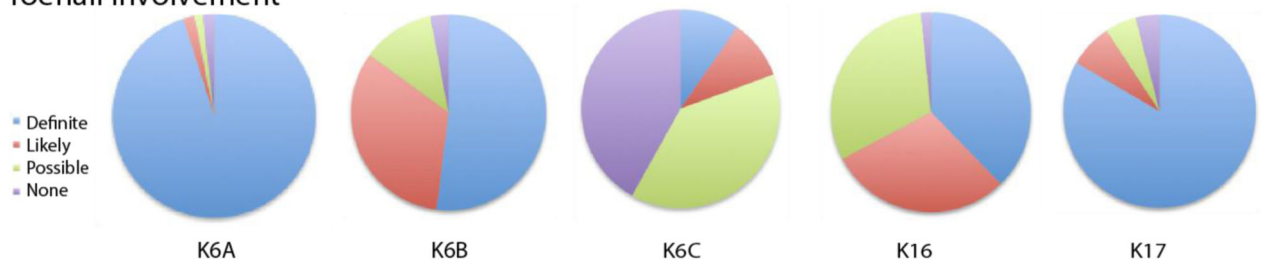

Number of toenails surgically removed

	KRT6A	KRT6B	KRT6C	KRT16	KRT17
>7 nails	20 (5%)	2 (2%)	0 (0%)	2 (1%)	5 (3%)
4-6 nails	4 (1%)	3 (3%)	0 (0%)	0 (0%)	1 (1%)
1-3 nails	13 (3%)	10 (11%)	1 (3%)	2 (1%)	10 (7%)
None	346 (90%)	74 (83%)	30 (97%)	310 (99%)	135 (89%)

Figure 3. Nail involvement by KRT gene groups

(A) Fingernail involvement by KRT gene groups. Ninety-six percent of K6A patients had definite or likely fingernail involvement, while as only 3% of K6C patients did. Though most patients did not have fingernails surgically removed, K6A patients had the highest percentage (10%) of patients who had at least 1 fingernail removed. (B) Toenail involvement by KRT gene groups. Ninety-seven percent of K6A patients had definite or likely toenail involvement compared to 19% of K6C patients. K6B patients had the highest percentage (16%) of patients who had at least 1 toenail removed.

*Definite involvement defined as >=7 nails reported to be thickened, likely as 4–6 nails, possible as 1–3 and none as 0.

a

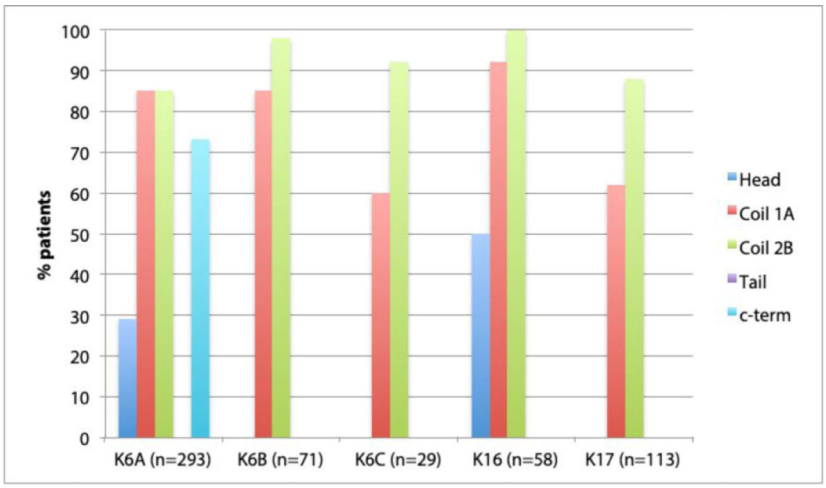

b

Mutation group	K6A	K6B	K6C	K16	K17
	n=336	*n*=86	*n*=29	*n*=58	*n*= 121
Pain often requires medication	80 (24%)	18 (21%)	8 (28%)	17 (29%)	20 (17%)
Very painful but no medication	139 (41%)	39 (44%)	16 (55%)	30 (52%)	40 (33%)
Somewhat painful	97 (29%)	29 (34%)	4 (14%)	9 (16%)	41 (34%)
Not painful	20 (6%)	0 (0%)	1 (3%)	2 (3%)	20 (17%)

C

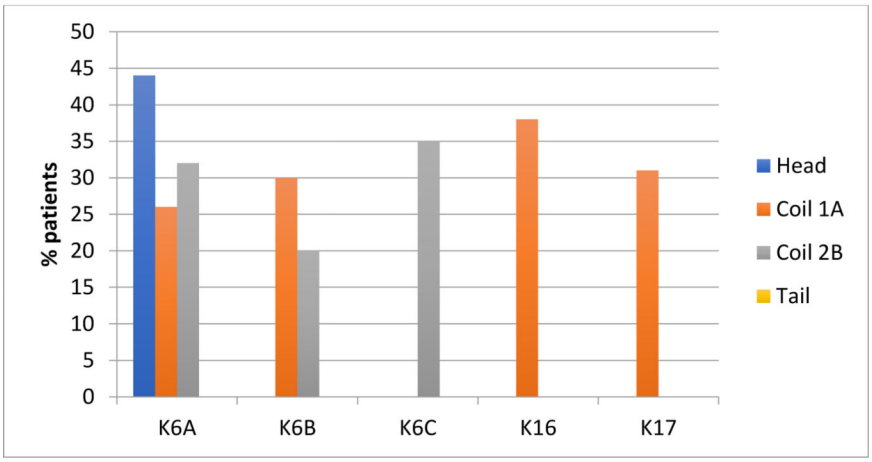

Figure 4. Functional impairment, severity of pain, and emotional impact associated with plantar keratoderma in PC by KRT gene group and subdomain

(A) Percentage* of PC patients reporting walking with pain or inability to walk without a walking aid grouped based on location of mutations within KRT gene. (B) Absolute number and percentage* of patients reporting each level of pain by KRT gene. (C) Percentage* of PC patients reporting an emotional or psychiatric issue by KRT gene and subdomain location of mutation.

*Percentages were calculated by dividing by *n* patients who responded for each question.

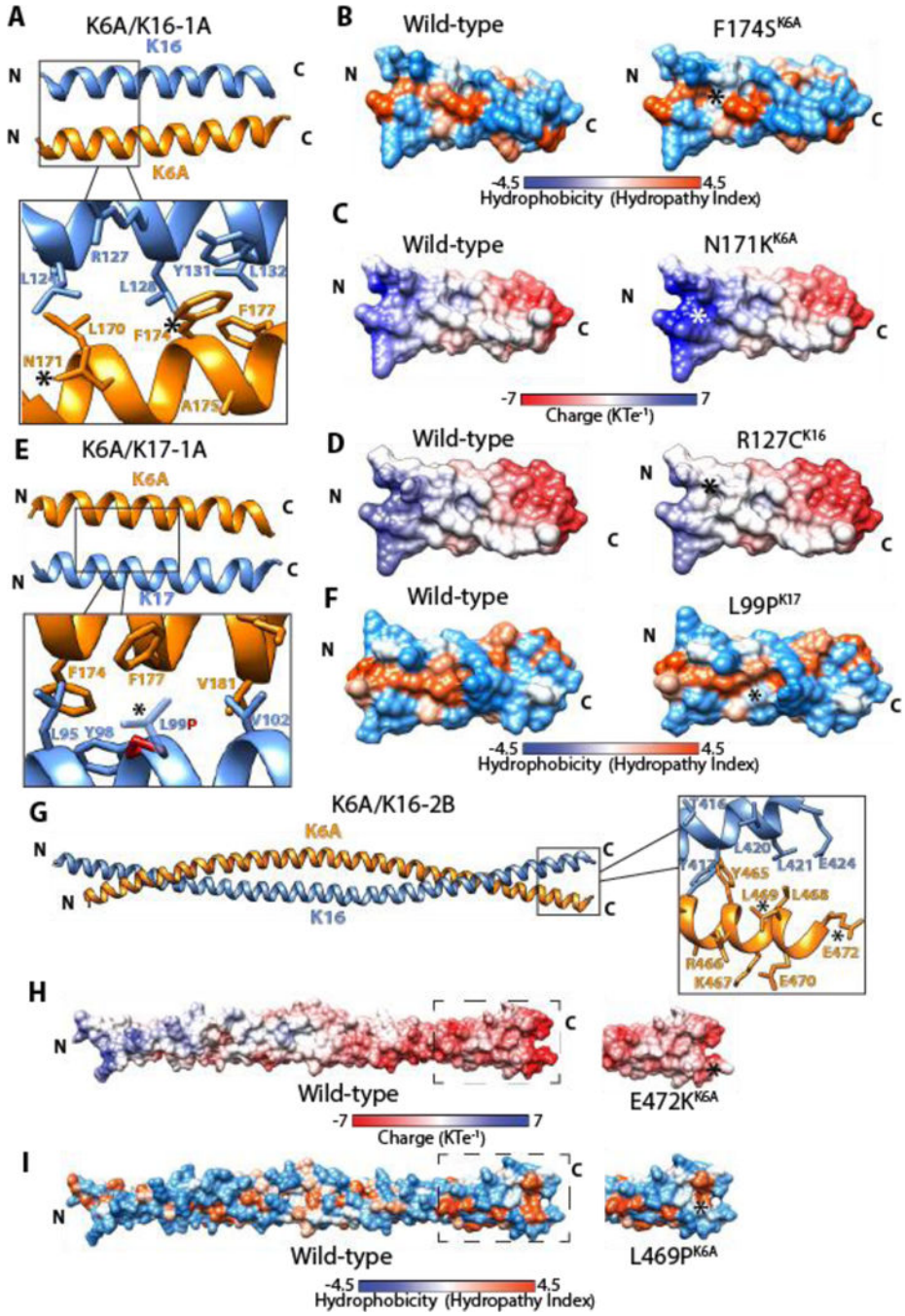

Figure 5. Molecular modeling of selected PC mutations.

Ribbon diagrams show overall structure of the K6A/K16–1A (A), K6A/K17–1A (E), and K6A/K16–2B (G) models with zoomed in view of regions containing residues involved in PC mutations (denoted by an asterisk). Comparisons of the hydrophobic surfaces of wild-type and mutated models harboring the F174S^{K6A} (B), L99P^{K17} (F) and L469P^{K6A} (I) show loss of hydrophobic surface area due to mutation. Comparisons of the charge

surfaces of wild-type and mutated models harboring the N171K^{K6A} (C), R127C^{K16} (D) and E472K^{K6A} (H) mutations show significant differences in surface charge.

Table 1.

Severity of palmar and plantar keratoderma by KRT gene groups

Mutation	K6A	K6B	K6C	K16	K17
Palmar keratoderma	***n*=339**	***n*=76**	***n*=23**	***n*=43**	***n*=133**
Always	109 (32%)	19 (25%)	4 (17%)	25 (58%)	22 (17%)
Sometimes	44 (13%)	8 (11%)	1 (4%)	3 (7%)	25 (19%)
Seldom	62 (18%)	16 (21%)	5 (22%)	7 (16%)	30 (23%)
Never	124 (37%)	33 (43%)	13 (57%)	8 (19%)	56 (42%)
Plantar keratoderma	***n*=361**	***n*=88**	***n*=29**	***n*=59**	***n*=143**
Always	309 (86%)	85 (97%)	27 (93%)	59 (100%)	100 (70%)
Sometimes	15 (4%)	1 (1%)	2 (7%)	0 (0%)	15 (10%)
Seldom	6 (2%)	0 (0%)	0 (0%)	0 (0%)	7 (5%)
Never	31 (9%)	2 (2%)	0 (0%)	0 (0%)	21 (15%)

[*] % of patients calculated by dividing by total *n* number of patients who responded for each question

[*] Always described as keratoderma never completely going away, sometimes as hands/feet clear up completely at times, and seldom as usually clear of symptoms

Table 2.

Associated clinical manifestations grouped based on KRT gene affected

Mutation	K6A (*n*=383)	K6B (*n*=89)	K6C (*n*=31)	K16 (*n*=61)	K17 (*n*=150)
Alopecia	37 (11%)	11 (16%)	4 (16%)	10 (16%)	22 (16%)
Oral leukokeratosis	334 (87%)	21 (24%)	7 (28%)	17 (28%)	37 (25%)
Natal or prenatal teeth	17 (4%)	0 (0%)	3 (12%)	1 (2%)	113 (76%)
Hyperhidrosis	125 (34%)	19 (22%)	8 (35%)	12 (20%)	47 (32%)
Steatocystoma or pilosebaceous cysts	136 (36%)	44 (50%)	5 (19%)	8 (14%)	114 (76%)
Follicular hyperkeratosis	191 (50%)	34 (39%)	0 (0%)	8 (14%)	91 (61%)